ORIGINAL ARTICLE

Radius of curvature at the talocrural joint surface: inference of subject-specific kinematics

Shuhei Nozaki[1,2] · Kota Watanabe[2] · Takuya Kato[1] · Tsuyoshi Miyakawa[1,3] · Tomoaki Kamiya[1,3] · Masaki Katayose[2]

Abstract

Purpose The coupled behavior of talocrural joint motion is primarily determined by the morphological features of the talar trochlea and tibiofibular mortise. Features of the radius of curvature of the talocrural joint, however, remain unclear. The objectives of this study were to evaluate the radius of curvature at the mid, medial, and lateral regions of both the talar trochlea and the tibial plafond, and to estimate subject-specific kinematics of the talocrural joint.

Methods Computed tomography images of 44 subjects with healthy talocrural joints were assessed by creating three-dimensional bone models. The radii of curvature of the anterior and posterior regions at the mid, medial, and lateral regions of both the talar trochlea and the tibial plafond were calculated. Hypothetical dorsiflexion and plantarflexion axes of the talocrural joint were estimated from the shape of the talar trochlea. Orientations and distances of these axes were calculated.

Results At both the talar trochlea and the tibial plafond, the anteromedial and posteromedial radii exhibited the largest coefficients of variation. The anterior-to-posterior radius ratio (APRR) of the medial talar trochlea significantly correlated with the mid APRR, anterior medial-to-lateral radius ratio (MLRR), and posterior MLRR of the trochlea ($r = 0.45$, 0.52, -0.60, respectively, and all $P < 0.01$).

Conclusions The asymmetric shape of the medial talar trochlea seems to determine a fixed or changing axis of rotation at the talocrural joint. This subject-specific rotational axis of the talocrural joint should be considered in the management of patients with ankle injuries.

Keywords Talus · Tibia · Radius · Image-based bone models · Translation · Sliding

Introduction

The talocrural joint produces six degree-of-freedom coupled motions during ankle dorsiflexion and plantarflexion [5–9, 19]. Although these coupled motions result from the interaction between the morphology of the articular surface, ligament constraints, and total force through the adjacent joints, the basic passive kinematic patterns are primarily determined by the morphology of the articular surface of the talar trochlea and tibial plafond.

The axis of rotation at the talocrural joint is considered to orient due to the asymmetric shape of the medial and lateral talar trochlea [7, 15]. In particular, the lateral radius is larger compared with the medial radius at the anterior talar trochlea [4, 11], which orient the talocrural joint axis downward and laterally during ankle dorsiflexion [9]. On the other hand, at the posterior talar trochlea, 60% of the talus exhibits the larger medial radius compared with the lateral radius, while the remainder exhibits the smaller medial radius [11]. This bilateral asymmetry of the posterior talar trochlea is considered to orient the talocrural joint axis downward and medially or laterally during ankle plantarflexion [9].

In addition to the orientation of the axes, the positional change of the axis of the talocrural joint, which should induce the translation and sliding motion of the talus, is considered to occur due to the asymmetry between the

✉ Shuhei Nozaki
  nozakis@sapmed.ac.jp

1 Center of Sports Medicine, Hokkaido Obihiro Kyokai Hospital, South-9, East-5, Obihiro, Hokkaido 080-0805, Japan

2 Second Division of Physical Therapy, School of Health Sciences, Sapporo Medical University, South-1, West-17, Chu-Ou-Ku, Sapporo, Hokkaido 060-8556, Japan

3 Department of Orthopaedic Surgery, School of Medicine, Sapporo Medical University, South-1, West-16, Chu-Ou-Ku, Sapporo, Hokkaido 060-8543, Japan

anterior and posterior radii of the talar trochlea. In fact, the asymmetry between the anterior and posterior radii at the mid-region of the talar trochlea should induce anteroposterior translation of the talus relative to the tibial plafond throughout the range of motion of the ankle by separating the dorsiflexion and plantarflexion axes at the central level of the talar body. At the medial and lateral talar trochlea, the asymmetry between anterior and posterior radii should produce the anteroposterior sliding motion of the medial and lateral compartments of the trochlear surface throughout ankle dorsiflexion and plantarflexion motions. However, the features of asymmetry between the anterior and posterior radii at the mid, medial, and lateral talar trochlea remain unclear. Furthermore, although such translation and sliding motion of the talus at the talocrural joint would be permitted by the structural feature of the tibial plafond, the quantitative values of the normal radii of the mid, medial, and lateral tibial plafond have not been assessed in relation to the counterparts of the talar trochlea.

The features of the radii at the talar trochlea and tibial plafond are crucial to understanding the subject-specific kinematics of the talocrural joint, which provide essential information for the management of patients with various ankle injuries. The purposes of the present study were (1) to assess normal variants in the radii of the six regions at both the talar trochlea and tibial plafond and (2) to estimate subject-specific orientations of the dorsiflexion and plantarflexion axes of the talocrural joint and the distances between these axes from the morphology of the talar trochlea.

Materials and methods

Subject selection

Subjects presenting with foot or ankle symptoms who underwent foot and ankle-computed tomography (CT) scans and were diagnosed with no talocrural pathology between January 1, 2006, and August 31, 2017, were identified within the Hokkaido Obihiro Kyokai Hospital (HOKH) and Sapporo Medical University Hospital (SMUH) databases. Subjects below 20 years of age and patients with any talocrural pathology (fracture, osteoarthritis, osteochondral lesion, and others) were excluded. History of the subjects' previous ankle injury was unknown. After exclusion, 44 talocrural joints (22 right and 22 left joints) in 8 women and 36 men [mean age 48.0 (SD 18.0) years; age range 23–84 years] were enrolled in this study. CT images collected from HOKH were acquired using an Aquilion Multi-detector CT scanner (Toshiba Medical Systems, Otawara, Japan). The acquisition parameters were: tube voltage 120 kVp, tube current 10–500 mA, rotation time 1.00 s per 360°, pitch 53.0, collimation 32 mm, matrix 512×512 pixels, slice thickness

0.5–2.00 mm, field of view 240 mm. CT images collected from SMUH were acquired using an Aquilion PRIME CT scanner (Toshiba Medical Systems, Otawara, Japan). The acquisition parameters were: tube voltage 120 kVp, tube current 100 mA, rotation time 0.5 s per 360°, matrix 512×512 pixels, slice thickness 1.00 mm, field of view 240 mm. Approval of this study was obtained from the ethics committee of the Obihiro Kyokai Hospital (#2017-12) and Sapporo Medical University Hospital (#29-2-46).

Reconstruction of the three-dimensional bone models

Three-dimensional (3D) bone models of the talocrural joint were reconstructed from the CT images by one experienced physical therapist (S.N.) possessing 7 years' experience with 3D reconstruction and morphometric analysis of the foot and ankle joints. The CT images were segmented by standardized thresholding to separate the bone contrast from the surrounding contrast levels (threshold values, minimum 226; maximum 2312) using Mimics (version 9.0, Materialise Inc., Leuven, Belgium). The 3D geometric models of the distal tibia and talus were reconstructed from the CT images, and the wrapping processing was done on the models. Morphometric analysis of the distal tibia and talus was then performed using 3-matic (version 9.0, Materialise Inc., Leuven, Belgium).

Tibial plafond radius of curvature

To measure the radius of the tibial plafond, an anatomical coordinate system (ACS) was defined as follows: four anatomical landmarks on the tibial plafond were identified (Fig. 1). First, the tibial plafond origin (O_p) coincided with the center of inertia of the region of the tibial plafond (Fig. 1). The three orthogonal planes were then created as follows: the transverse plane of the tibial plafond was defined as a plane orthogonal to a line orthogonal to the extracted surface of the tibial plafond (Fig. 2a). A plane perpendicular to the transverse plane and parallel to the line connecting anteromedial and anterolateral edges of the tibial plafond was defined as the coronal plane (Fig. 2a). The sagittal plane was defined as a plane perpendicular to both the transverse and coronal planes (Fig. 2a). The $X_p Y_p Z_p$ axes were defined as shown in Fig. 2b.

The tibial plafond radii of curvature were measured as follows: first, the three near-coronal sections were created through the tibial plafond (Fig. 3). Then, the five near-sagittal sections perpendicular to the transverse plane were defined through the tibial plafond as anteromedial, posteromedial, anterolateral, posterolateral, and mid-sagittal sections (Fig. 3). In the anteromedial section, a circle passing through the anteromedial top and mid-medial top and
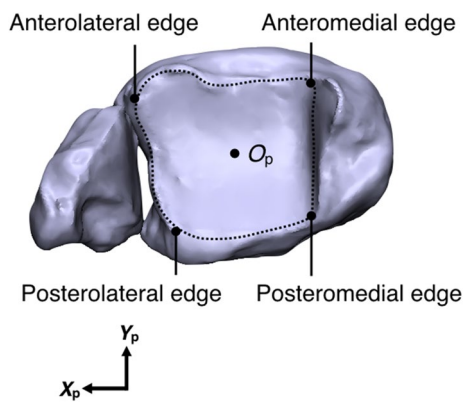
Fig. 1 Anatomical landmarks and origin of the tibial plafond. The anteromedial, posteromedial, anterolateral, and posterolateral edges were identified. The tibial plafond origin (O_p) coincided with the center of inertia of the region of the tibial plafond that was manually extracted by tracking the visible borders of the subchondral bone surfaces (dotted line)

the midpoint of these two tops projected onto the tibial plafond contour (anteromedial midpoint) was created, and the radius of this circle was calculated as the anteromedial radius (Fig. 4a). Second, in the posteromedial section, a circle passing through the mid-medial top and postero-medial top of the tibial plafond and the midpoint of these two tops projected onto the tibial plafond contour (pos-teromedial midpoint) was created, and the radius of this circle was calculated as the posteromedial radius (Fig. 4b). Third, in the anterolateral section, a circle passing through the anterolateral top and mid-lateral top and the midpoint of these two tops projected onto the tibial plafond con-tour (anterolateral midpoint) was created, and the radius of this circle was calculated as the anterolateral radius (Fig. 4a). Fourth, in the posterolateral section, a circle passing through the mid-lateral and posterolateral top and the midpoint of these two tops projected onto the tibial plafond contour (posterolateral midpoint) was created, and the radius of this circle was calculated as the posterolateral radius (Fig. 4b). Finally, in the mid-sagittal section, a cir-cle passing through the most anterior and superior points and the midpoint of these two tops projected onto the tibial plafond contour (anterior midpoint) was created, and the radius of this circle was calculated as the mid-anterior radius (Fig. 4c). The mid-posterior radius was measured via the same procedure (Fig. 4c).

The anterior-to-posterior radius ratios (APRRs) of the medial, lateral, and mid-tibial plafond were defined as the ratio of the anteromedial to the posteromedial radius, ante-rolateral to the posterolateral radius, and mid-anterior to the mid-posterior radius, respectively. The medial-to-lateral radius ratios (MLRRs) of the anterior and posterior tibial plafond were calculated as the ratio of the anteromedial to
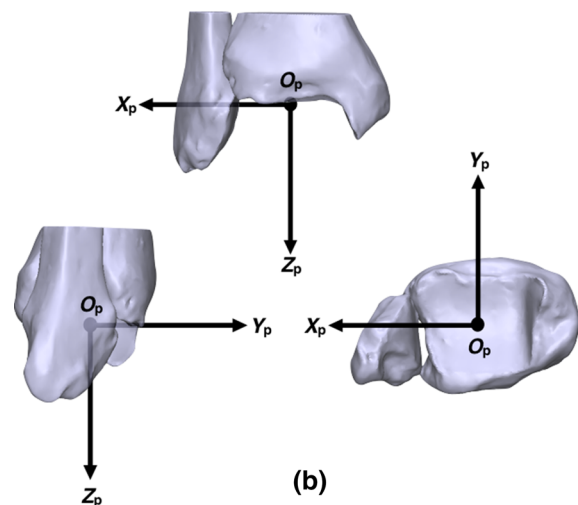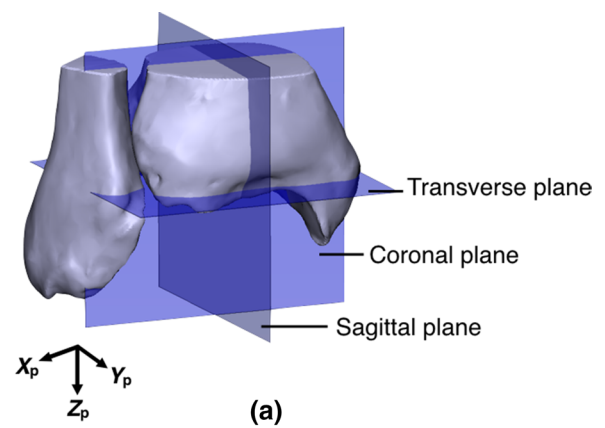

Fig. 2 Three-orthogonal planes (**a**) and the anatomical coordinate system (**b**) of the tibial plafond. The X_p axis was defined as the line perpendicular to the sagittal plane and passing through O_p, pointing laterally. The Y_p axis was defined as the line perpendicular to the cor-onal plane and passing through O_p, pointing anteriorly. The Z_p axis was formed as the cross-product of the X_p axis and Y_p axis, pointing downward

the anterolateral radius of curvature and the posteromedial to the posterolateral radius of curvature, respectively.

Talar trochlea radius of curvature

The process of measuring radii of curvature of the talar trochlea followed a previously described procedure [11]. Briefly, at first, an ACS of the talus was embedded as follows: the transverse plane was parallel to both the line passing through the superior edges of the facets of the medial and lateral sides of trochlea and the line passing through the anterior and posterior edges of the medial facet of the trochlea. The coronal plane was parallel to the line passing through the anteromedial and ante-rolateral edges of the trochlea and perpendicular to the transverse plane. The sagittal plane was perpendicular to
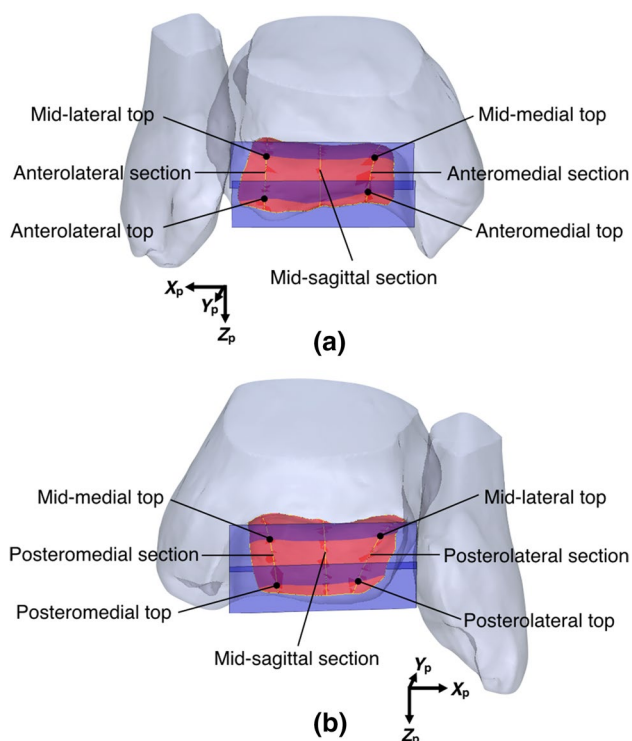
Fig. 3 Three near-coronal sections and five near-sagittal sections through the tibial plafond. Three near-coronal sections were created to individually contain anteromedial and anterolateral edges of the tibial plafond, midpoints of the anteromedial and posteromedial edges and anterolateral and posterolateral edges, and posteromedial and posterolateral edges. On each of the three near-coronal sections, the most superior points at the medial and lateral edges of the tibial plafond were identified and defined as the anteromedial top, mid-medial top, posteromedial top, anterolateral top, mid-lateral top, and posterolateral top. An anteromedial section was defined to contain the anteromedial top and mid-medial top (**a**). A posteromedial section was then defined to contain the mid-medial top and posteromedial top (**b**). An anterolateral section was defined to contain the anterolateral top and mid-lateral top (**a**). A posterolateral section was defined to contain the mid-lateral top and posterolateral top (**b**). A mid-sagittal section was created by cutting the tibial plafond along the Y_pZ_p plane
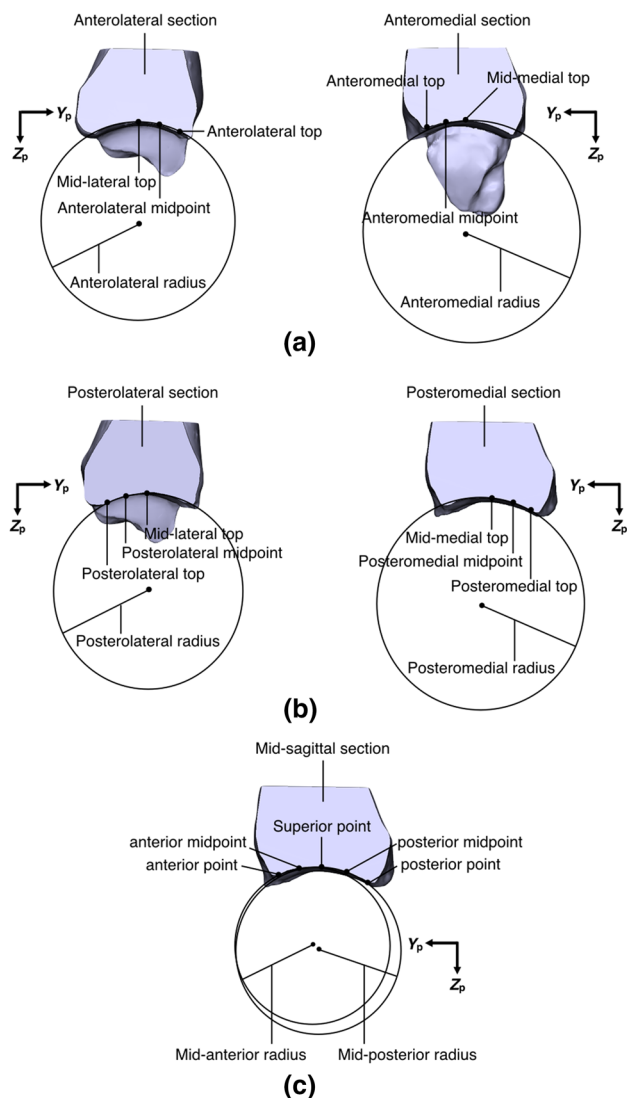

Fig. 4 Five near-sagittal sections and radii of curvature of the tibial plafond. On each section, anteromedial, posteromedial, anterolateral, posterolateral, mid-anterior, and mid-posterior radii of curvature were calculated

Orientation of dorsiflexion and plantarflexion axes

The dorsiflexion axis was defined as a line through the centers of the anteromedial and anterolateral circles of the talar trochlea. The plantarflexion axis was defined as a line through the centers of the posteromedial and posterolateral circles of the trochlea. To assess the orientation of the dorsiflexion and plantarflexion axes, the inclination and deviation angles of these axes were calculated following a previously described procedure [11]. The inclination angle was defined as the angle between the dorsiflexion or plantarflexion axis and X_tY_t plane (Fig. 8a). The deviation angle was defined as the angle between the dorsiflexion or plantarflexion axis and X_tZ_t plane (Fig. 8b).

both the transverse and coronal planes. The talar origin (O_t) was determined following the process reported in a previous study [19]. The $X_tY_tZ_t$ axes were defined as shown in Fig. 5. Then, five near-sagittal sections were determined: the anteromedial, posteromedial, anterolateral, posterolateral, and mid-sagittal sections (Fig. 6). On each near-sagittal section, anteromedial, posteromedial, anterolateral, posterolateral, mid-anterior, and mid-posterior circles were created, and radii of curvature of each circle were calculated (Fig. 7). The APRR and MLRR of the talar trochlea were calculated in the same way as the counterpart of the tibial plafond.
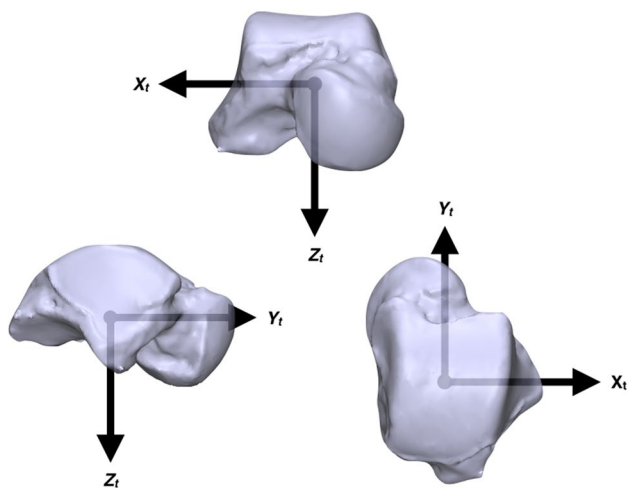
Fig. 5 The anatomical coordinate system of the talus. The X_t axis was defined as the line perpendicular to the sagittal plane and passing through O_t, pointing laterally. The Y_t axis was defined as the line perpendicular to the coronal plane and passing through O_t, pointing anteriorly. The Z_t axis was formed as a cross-product of the X_t axis and Y_t axis, pointing downward
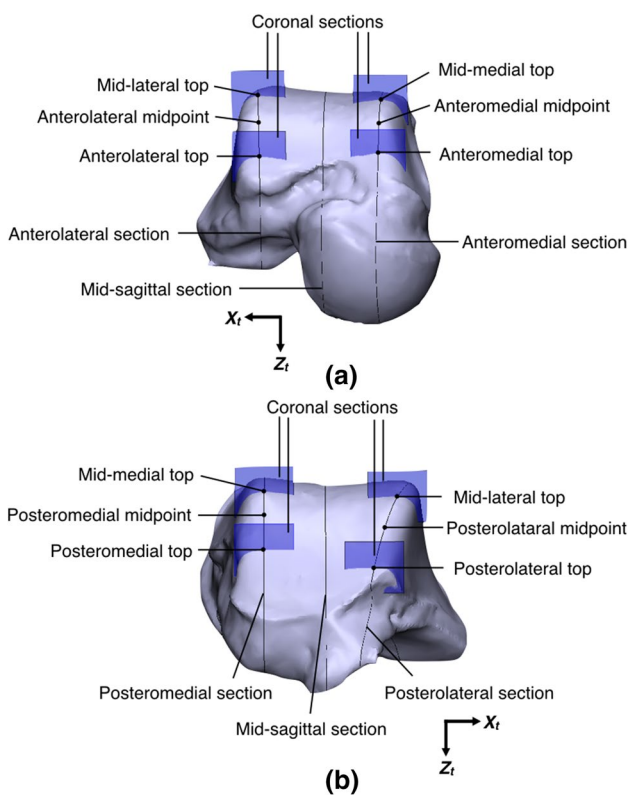

Fig. 6 Five near-sagittal sections through the talar trochlea. The anteromedial section contained the anteromedial and mid-medial tops (**a**). The posteromedial section contained the mid-medial and posteromedial tops (**b**). The anterolateral section contained the anterolateral and mid-lateral tops (**a**). The posterolateral section contained the mid-lateral and posterolateral tops (**b**). All sections were perpendicular to the transverse plane. The mid-sagittal section was created by cutting the talar trochlea along the Y_tZ_t plane
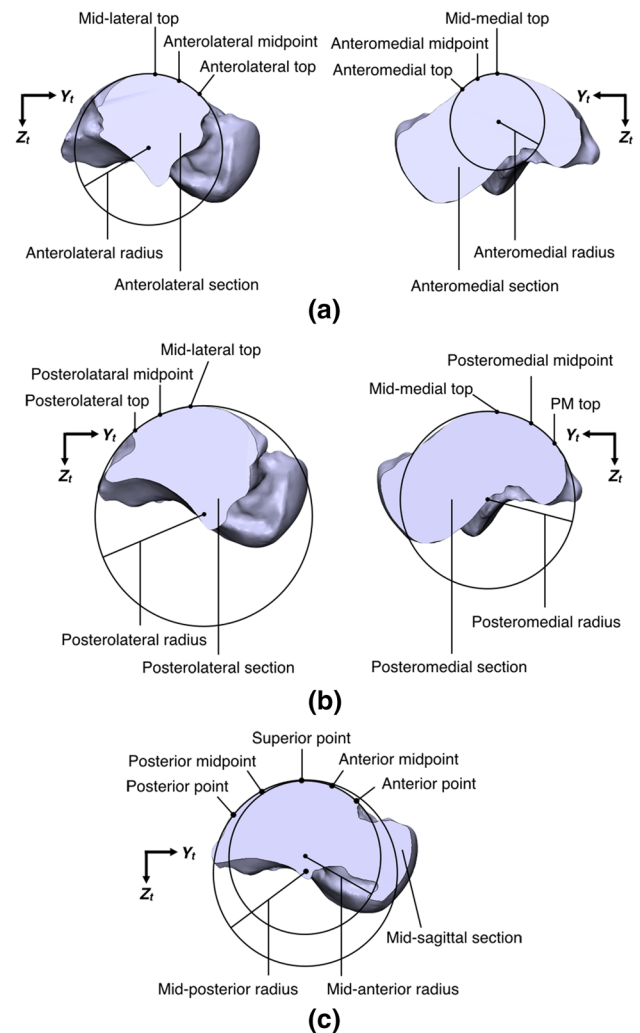

Fig. 7 Radii of curvature of the talar trochlea. The anteromedial circle contained the anteromedial and mid-medial tops and anteromedial midpoint (**a**). The posteromedial circle contained the mid-medial and PM tops and posteromedial midpoint (**b**). The anterolateral circle contained the anterolateral and mid-lateral tops and anterolateral midpoint (**a**). The posterolateral circle contained the mid-lateral and posterolateral tops and posterolateral midpoint (**b**). The mid-anterior circle contained the most anterior point, most superior point, and midpoint of the most anterior and superior points of the trochlea (**c**). The mid-posterior circle contained the most posterior point, most superior points, and midpoint of the most posterior and superior points of the trochlea (**c**)

Distance between dorsiflexion and plantarflexion axis

The distance between dorsiflexion and plantarflexion axes was assessed at the medial, mid, and lateral parts, respectively (Fig. 9). The medial distance was measured from the anteromedial center to the posteromedial center of the talar trochlea. The mid distance was defined as the distance between intersection points of the dorsiflexion and
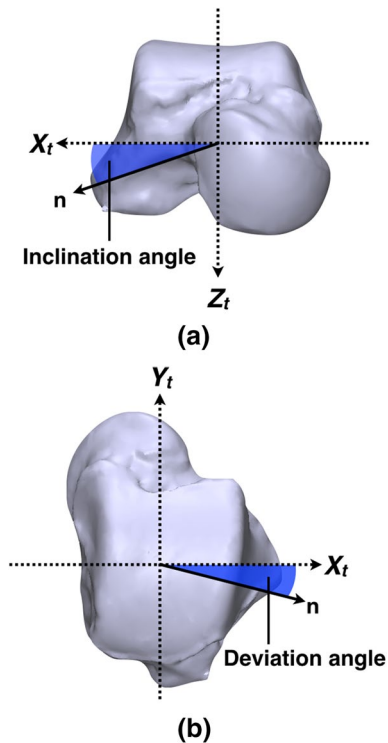
Fig. 8 Inclination (**a**) and deviation (**b**) angles of the dorsiflexion and plantarflexion axes. The direction of the axis is represented by the normal vector *n*. A positive value of the inclination angle indicates an inferiorly oriented axis in a lateral direction, and a positive value of the deviation angle indicates a laterally oriented axis in a posterior direction

plantarflexion axis with the Y_tZ_t plane. The lateral distance was measured from the anterolateral center to the posterolateral center of the talar trochlea. The absolute values of distance between dorsiflexion and plantarflexion axes were normalized using the anteroposterior diameter of the talar trochlea (the distance from the most anterior point to the
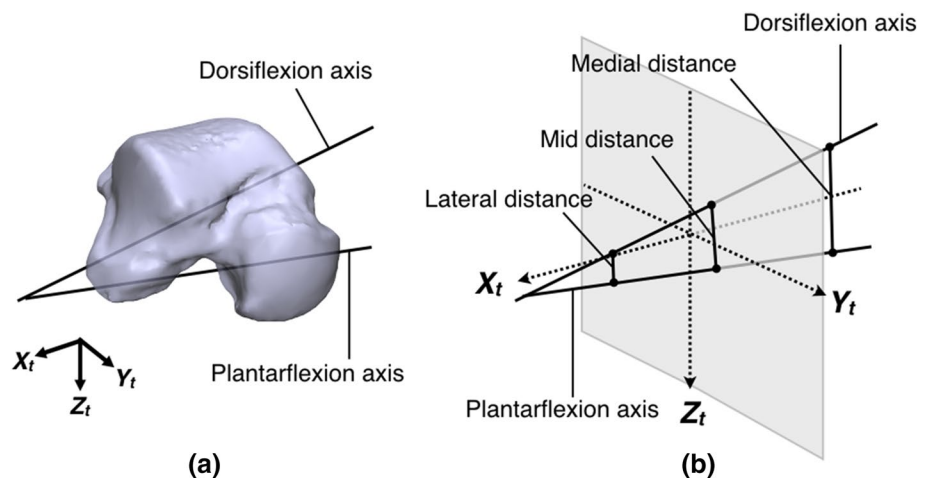
most posterior point on the talar trochlea) for the following correlation analysis.

Statistical analysis

All measurements were performed twice by one observer (S.N.). The average of two trials was used for statistical analysis. Measurement repeatability of the tibial and talar radius, orientation of the dorsiflexion and plantarflexion axes, and distances between these two axes was examined using the intraclass correlation coefficient (ICC) and the standard error of measurement (SEM). Intra-observer repeatability for the two measurements in 44 subjects was assessed by ICC model 1,1. Inter-observer repeatability was assessed in 25 randomly selected subjects using ICC model 2,1 by two independent physical therapists (S.N., T.K.). The repeatability was assumed to be good for ICC > 0.75, moderate for ICC of 0.50–0.75, and poor for ICC < 0.50, using previously established criteria [13]. The radii of curvature of the six regions at the tibial plafond and talar trochlea were independently analyzed using the Friedman test (factor: region). When main effects were found, multiple comparisons using the Wilcoxon signed-rank test were performed. In addition, the Wilcoxon signed-rank test was used for the comparison of the radii of curvature at each region between the tibial plafond and talar trochlea. Correlations among the APRRs and MLRRs of the talar trochlea were assessed using Spearman's rank correlation coefficient. Correlations between the MLRRs of the talar trochlea and orientation angles of the dorsiflexion and plantarflexion axis were assessed using Spearman's rank correlation coefficient. Correlations between the APRRs of the talar trochlea and normalized distances between the dorsiflexion and plantarflexion axis were also analyzed using Spearman's rank correlation coefficient. The distance between the dorsiflexion and plantarflexion axes at three parts (medial, mid, and lateral) was analyzed using the Friedman test (factor: part). When

Fig. 9 The dorsiflexion and plantarflexion axes (**a**) and the distance between these axes (**b**). The intersection points of the dorsiflexion and plantarflexion axes with the Y_tZ_t plane were identified (**b**). The distance between these intersection points was defined as the distance between dorsiflexion and plantarflexion axes (**b**)

main effects were found, multiple comparisons using the Wilcoxon signed-rank test were performed. The statistical significance level was set at P value < 0.05 for all analyses, while Bonferroni correction was used where appropriate. All statistical analyses were performed using SPSS software version 19.0 (SPSS Japan Inc., Tokyo, Japan).

Results

Intra-observer and inter-observer repeatability

Good intra-observer repeatability (ICC1,1 > 0.75) was found in all measurements except for the mid distance between dorsiflexion and plantarflexion axes (Tables 1, 2, 3). Although the ICC1,1 for the mid distance between dorsiflexion and plantarflexion axes was moderate, good intra-observer repeatability was found when the average of two trials was used for the analysis. Good inter-observer repeatability (ICC2,1 > 0.75) was found in all measurements except for the posterolateral radius of the tibial plafond and the lateral distance between dorsiflexion and plantarflexion axes (Tables 1, 2, 3).

Tibial and talar radii of curvature

On the tibial plafond, anteromedial and posteromedial radii exhibited the largest coefficient of variation (Table 1). At the anterior tibial plafond, the anteromedial radius was

significantly larger compared with the mid-anterior and anterolateral radius by a mean difference of 10.3 (SD 15.5) and 9.2 (SD 14.8) mm, respectively (P < 0.001; Table 1). At the mid tibial plafond, the mid-anterior radius was significantly smaller compared with the mid-posterior radius by a mean difference of 4.7 (SD 6.8) mm (P < 0.001; Table 1).

On the talar trochlea, anteromedial and posteromedial radii also exhibited the largest coefficient of variation (Table 2). The anterior radius was significantly smaller compared with the posterior radius at all the medial, mid, and lateral talar trochlea by a mean difference of 6.9 (SD 5.5) mm, 3.2 (SD 2.6) mm, and 2.6 (SD 4.0) mm, respectively (P < 0.001; Table 2). At the medial talar trochlea, the APRRs in 40 (91%) samples were less than 1.0. At the mid talar trochlea, the APRRs in 38 (86%) samples were less than 1.0, and the remainder (14%) were more than 1.0. At the lateral talar trochlea, the APRRs of the talar trochlea in 29 (66%) samples were less than 1.0, and the remainder (34%) were more than 1.0. At the anterior talar trochlea, the anteromedial and mid-anterior radius was significantly smaller compared with the anterolateral radius by a mean difference of 5.5 (SD 2.8) and 4.7 (SD 2.4) mm, respectively (P < 0.001; Table 2). At the posterior trochlea, the mid-posterior radius was significantly smaller compared with the posteromedial and posterolateral radius by a mean difference of 2.9 (SD 4.4) and 4.1 (SD 3.9) mm, respectively (P < 0.001; Table 2). The anterior MLRRs of the talar trochlea in 42 (95%) samples were less than 1.0. The posterior MLRRs of the talar trochlea in 25 (57%) samples were less

Table 1 Radii of curvature of the tibial plafond

Variable	Mean (SD)	Range	CV (%)	Intraobserver		Interobserver	
				ICC1,1 (95% CI)	SEM	ICC2,1 (95% CI)	SEM
Radius of curvature							
Anteromedial radius (mm)	33.9 (14.5)*,†	13.4–86.6	42.9	0.974 (0.953–0.986)	0.39	0.789 (0.581–0.901)	1.83
Mid-anterior radius (mm)	23.6 (5.2)‡	15.3–47.1	22.2	0.975 (0.955–0.986)	0.13	0.946 (0.879–0.976)	0.34
Anterolateral radius (mm)	24.7 (4.6)	16.4–41.9	18.6	0.909 (0.840–0.949)	0.43	0.777 (0.555–0.895)	1.15
Posteromedial radius (mm)	29.5 (11.0)	15.2–64.4	37.1	0.971 (0.948–0.984)	0.32	0.892 (0.773–0.951)	1.26
Mid-posterior radius (mm)	28.3 (6.9)	18.3–56.8	24.4	0.958 (0.925–0.977)	0.29	0.949 (0.888–0.977)	0.41
Posterolateral radius (mm)	25.5 (5.0)	14.4–39.1	19.5	0.917 (0.854–0.954)	0.43	0.689 (0.345–0.859)	1.74
Anterior-to-posterior radius ratio							
Medial trochlea	1.24 (0.62)	0.45–3.01	49.8				
Mid trochlea	0.86 (0.20)	0.53–1.59	23.8				
Lateral trochlea	1.00 (0.24)	0.67–1.77	24.3				
Medial-to-lateral radius ratio							
Anterior trochlea	1.40 (0.62)	0.55–3.22	44.2				
Posterior trochlea	1.19 (0.43)	0.57–2.35	36.4				

CV coefficient of variation, *ICC* intraclass correlation coefficient, *SEM* standard error of measurement

*P < 0.001 compared with the mid-anterior radius

†P < 0.001 compared with the anterolateral radius

‡P < 0.001 compared with the mid-posterior radius

Table 2 Radii of curvature of the talar trochlea

Variable	Mean (SD)	Range	CV (%)	Intraobserver		Interobserver	
				ICC1,1 (95% CI)	SEM	ICC2,1 (95% CI)	SEM
Radius of curvature							
Anteromedial radius (mm)	17.9 (3.0)*,†	13.2–26.4	16.7	0.941 (0.894–0.967)	0.18	0.940 (0.870–0.973)	0.21
Mid-anterior radius (mm)	18.7 (2.2)‡,§	15.2–24.9	11.7	0.956 (0.922–0.976)	0.10	0.895 (0.778–0.952)	0.26
Anterolateral radius (mm)	23.4 (2.8)‖	18.2–29.7	12.1	0.958 (0.924–0.977)	0.12	0.931 (0.850–0.969)	0.22
Posteromedial radius (mm)	24.8 (5.0)¶	15.8–47.9	20.3	0.967 (0.941–0.982)	0.17	0.958 (0.908–0.981)	0.23
Mid-posterior radius (mm)	21.9 (2.3)**	17.8–27.9	10.7	0.982 (0.967–0.990)	0.04	0.892 (0.772–0.951)	0.27
Posterolateral radius (mm)	26.0 (4.1)	18.2–36.6	15.7	0.948 (0.907–0.971)	0.22	0.891 (0.771–0.950)	0.45
Anterior-to-posterior radius ratio							
Medial trochlea	0.74 (0.16)	0.37–1.12	21.5				
Mid trochlea	0.86 (0.11)	0.67–1.18	13.2				
Lateral trochlea	0.92 (0.14)	0.67–1.25	15.5				
Medial-to-lateral radius ratio							
Anterior trochlea	0.77 (0.11)	0.59–1.04	14.3				
Posterior trochlea	0.97 (0.20)	0.55–1.82	20.9				

CV coefficient of variation, *ICC* intraclass correlation coefficient, *SEM* standard error of measurement

*$P < 0.001$ compared with the anterolateral radius

**$P < 0.001$ compared with the posterolateral radius

†$P < 0.001$ compared with the posteromedial radius

‡$P < 0.001$ compared with the anterolateral radius

§$P < 0.001$ compared with the mid-posterior radius

‖$P < 0.001$ compared with the posterolateral radius

¶$P < 0.001$ compared with the mid-posterior radius

Table 3 Orientation of the dorsiflexion and plantarflexion axes and distances between these axes

Variable	Mean (SD)	Range	CV (%)	Intraobserver		Interobserver	
				ICC1,1 (95% CI)	SEM	ICC2,1 (95% CI)	SEM
Dorsiflexion axis							
Inclination angle (°)	13.4 (6.9)	− 1.7 to 27.4	51.8	0.886 (0.802–0.936)	0.82	0.842 (0.668–0.929)	1.10
Deviation angle (°)	6.9 (5.0)	− 3.1 to 16.7	72.9	0.890 (0.808–0.938)	0.58	0.936 (0.862–0.971)	0.33
Plantarflexion axis							
Inclination angle (°)	3.2 (13.3)	− 45.3 to 36.0	418.4	0.953 (0.917–0.974)	0.64	0.926 (0.840–0.966)	0.99
Deviation angle (°)	4.6 (5.3)	− 7.1 to 15.7	113.5	0.939 (0.891–0.966)	0.33	0.901 (0.791–0.955)	0.56
Distances							
Medial distance (mm)	7.1 (4.9)*,†	0.9 to 30.1	69.7	0.857 (0.753–0.919)	0.74	0.887 (0.761–0.948)	0.60
Mid distance (mm)	5.2 (3.1)	0.7 to 17.3	59.8	0.748 (0.583–0.854)	0.84	0.870 (0.730–0.940)	0.47
Lateral distance (mm)	4.7 (2.8)	1.1 to 12.5	59.8	0.848 (0.739–0.914)	0.45	0.713 (0.450–0.863)	0.76

CV coefficient of variation, *ICC* intraclass correlation coefficient, *SEM* standard error of measurement

*$P < 0.001$ compared with the mid distance

†$P < 0.001$ compared with the medial distance

than 1.0, and those in the remainder (43%) were more than 1.0. Correlation coefficients among MLRRs and APRRs in the talar trochlea are presented in Table 4. The medial APRR correlated with mid APRR, anterior MLRR, and posterior MLRR ($r = 0.45$ and $P < 0.001$, $r = 0.52$ and $P < 0.01$, $r = −0.60$ and $P < 0.001$, respectively; Table 4).

The difference of radii of curvature at each region between the tibial plafond and talar trochlea are shown in Fig. 10. At the medial region of the talocrural joint, the anteromedial and posteromedial radius of the tibial plafond was significantly larger compared with the counterparts of the talar trochlea by a mean difference of 16.0 (SD 14.8) and

Table 4 Correlation coefficients between medial-to-lateral radius ratio and anterior-to-posterior radius ratio of talar trochlea

| | Anterior-to-posterior radius ratio | | | | | | Medial-to-lateral radius ratio | | | |
| | Medial trochlea | | Mid trochlea | | Lateral trochlea | | Anterior trochlea | | Posterior trochlea | |
	r value	P value	r value	P value	r value	P value	r value	P value	r value	P value
Anterior-to-posterior radius ratio										
Medial trochlea	–	–	0.45	< 0.01	0.05	> 0.05	0.52	< 0.01	− 0.60	< 0.001
Mid trochlea	0.45	< 0.01	–	–	0.17	> 0.05	0.13	> 0.05	− 0.27	> 0.05
Lateral trochlea	0.05	> 0.05	0.17	> 0.05	–	–	− 0.40	< 0.01	0.50	< 0.01
Medial-to-lateral radius ratio										
Anterior trochlea	0.52	< 0.01	0.22	> 0.05	0.40	< 0.01	–	–	0.04	> 0.05
Posterior trochlea	− 0.60	< 0.001	− 0.27	> 0.05	0.50	< 0.01	− 0.22	> 0.05	–	–
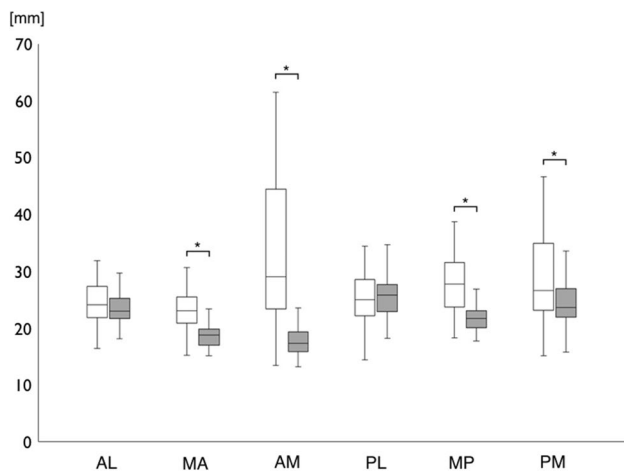
Fig. 10 Radius of the tibial plafond and talar trochlea at each region. A significant difference was found between the tibial plafond and talar trochlea at the anteromedial, mid-anterior, posteromedial, and mid-posterior regions. *AM* anteromedial, *MA* mid-anterior, *AL* anterolateral, *PM* posteromedial, *MP* mid-posterior, *PL* posterolateral. *$P < 0.001$

Table 5 Correlation coefficients between medial-to-lateral radius ratio and orientation angles of rotational axis

| Medial-to-lateral radius ratio | Inclination angle | | Deviation angle | |
	r value	P value	r value	P value
Anterior trochlea	− 0.93	< 0.001	–0.60	< 0.001
Posterior trochlea	− 0.98	< 0.001	0.67	< 0.001

4.7 (SD 9.4) mm, respectively ($P < 0.001$). At the mid region of the talocrural joint, the mid-anterior and mid-posterior radius of the tibial plafond was also significantly larger compared with the counterparts of the talar trochlea by a mean difference of 4.9 (SD 4.9) and 6.4 (SD 6.3) mm, respectively ($P < 0.001$). In contrast, at the lateral region, there were no differences of the radius between the tibial plafond and talar trochlea ($P > 0.01$).

Spatial position of dorsiflexion and plantarflexion axis

The orientation angles of the dorsiflexion and plantarflexion axis and the distances between these axes are shown in Table 3. The inclination and deviation angles of the dorsiflexion axis were positive values in 42 (95%) and 41 (93%)

samples, respectively. The inclination angle of the plantarflexion axis in 26 (59%) samples represented a positive value, while the remainder (41%) represented a negative value. The deviation angle of the plantarflexion angle in 34 (77%) samples represented a positive value, while the remainder (23%) represented a negative value. The inclination and deviation angles of the dorsiflexion axis were negatively correlated with the anterior MLRR of the talar trochlea ($r = −0.93$ and $P < 0.001$, $r = −0.60$ and $P < 0.001$, respectively; Table 5). The inclination and deviation angles of the plantarflexion axis were strongly correlated with the posterior MLRR of the talar trochlea ($r = −0.98$ and $P < 0.001$, $r = −0.67$ and $P < 0.001$, respectively; Table 5).

The medial distance between the dorsiflexion and plantarflexion axes was significantly larger compared with the mid and lateral distance by a mean difference of 1.9 (SD 2.7) and 2.4 (SD 5.7) mm, respectively ($P < 0.001$). The normalized medial distance was strongly correlated with the medial APRR of the talar trochlea ($r = −0.90$ and $P < 0.001$; Table 6). The normalized mid distance was significantly correlated with the mid APRR of the talar trochlea ($r = −0.37$ and $P < 0.05$; Table 6). The normalized lateral distance was significantly correlated with the lateral APRR of the talar trochlea ($r = −0.71$ and $P < 0.001$; Table 6).

Table 6 Correlation coefficients between anterior-to-posterior radius ratio and rotational axis distances

Anterior-to-posterior radius ratio	Normalized medial distance		Normalized mid distance		Normalized lateral distance	
	r value	P value	r value	P value	r value	P value
Medial trochlea	−0.90	<0.001				
Mid trochlea			−0.37	<0.05		
Lateral trochlea					−0.71	<0.001

Discussion

Three principal findings were obtained in this study. First, the medial talar trochlea exhibited the largest difference between the anterior and posterior radius, followed, in order, by the mid and lateral trochlea. Second, the tibial radius was significantly larger compared with the talar radius at the medial and mid region of the talocrural joint. Third, the medial APRR of the talar trochlea exhibited large individual variability and was correlated with the mid APRR, anterior MLRR, and posterior MLRR.

Several limitations of this study might affect the generalization of the three principal findings. First, the use of CT data to reconstruct 3D bone models would be a major confounding factor, as these models reflect only bone surface without cartilage layer. Although, to the best of our knowledge, cartilage thickness of the tibial plafond has not been reported, the thickness of the articular cartilage layer of the talar trochlea does not significantly vary between the medial, lateral, and central regions [1, 2]. In addition, the differences of the thickness of the articular cartilage between anterior and posterior regions of the talar trochlea are less than 0.6 mm [2]. Therefore, the use of 3D bone models without the articular cartilage layer are unlikely to affect the principal findings of this study. Second, using CT images that were acquired with the slice thickness of 2.0 mm in two subjects (4.5%) might have affected the accuracy of the measurements of the radius of curvature. However, the CT images of the remainder (95.5%) were acquired with the slice thickness of 0.5–1.0 mm, and the radius of curvature at both the tibial plafond and talar trochlea found in this study was reasonable according to the results in other studies [11, 14, 16, 18]. Third, this study enrolled 8 women and 36 men, and the relatively small number of female subjects may affect the generalization of the findings.

The present study revealed that the anterior radius was significantly smaller compared with the posterior counterpart at the mid talar trochlea. This smaller mid-anterior radius compared with the mid-posterior radius of the talar trochlea would induce the anterior and posterior translation during ankle dorsiflexion and plantarflexion motion, respectively. In fact, the mid distance between hypothetical dorsiflexion and plantarflexion axes was negatively correlated with the mid APRR of the talar trochlea. On the other hand, six (14%) subjects represented the larger mid-anterior radius compared with the mid-posterior radius of the talar trochlea. Such larger mid-anterior radius compared with the mid-posterior radius of the talar trochlea would produce posterior and anterior translation during ankle dorsiflexion and plantarflexion, respectively. This opposite direction of the anterior and posterior translation at the talocrural joint during ankle dorsiflexion and plantarflexion among subjects has also been observed in a previous study [9].

At the medial talar trochlea, the anterior radius was significantly smaller compared with the posterior radius, similar to the mid talar trochlea, and in agreement with a previous study [11]. Moreover, this relationship was applicable to almost all subjects (91%). The smaller anteromedial radius compared with the posteromedial radius would induce the posterior and anterior sliding of the medial talar trochlea relative to the medial tibial plafond during ankle dorsiflexion and plantarflexion, respectively. In fact, the medial distance between the hypothetical dorsiflexion and plantarflexion axes was negatively correlated with the medial APRR of the talar trochlea.

In addition to the medial trochlea, the smaller anterior radius compared with the posterior radius was also found at the lateral trochlea. The anterolateral radius was smaller than the posterolateral radius in 29 (66%) subjects, which would produce the sliding motion into the posterior and anterior direction of the lateral talar trochlea relative to the lateral tibial plafond during ankle dorsiflexion or plantarflexion, respectively. In contrast, a larger anterolateral radius compared with the posterolateral radius was found in 15 (34%) subjects, which would induce the sliding motion of the lateral talar trochlea into the anterior and posterior direction during ankle dorsiflexion and plantarflexion, respectively. Actually, the lateral distance between the hypothetical dorsiflexion and plantarflexion axes was negatively correlated with the lateral APRR of the talar trochlea. Although the variation in the sliding direction of the lateral trochlea was inferred as mentioned above, the degrees of the sliding motion of the lateral trochlea would be considerably small compared with the medial trochlea according to the smaller lateral distance between the hypothetical dorsiflexion and plantarflexion axes (Table 3). Therefore, the lateral talar trochlea would represent nearly pure spinning motion during ankle dorsiflexion and plantarflexion motions.

The tibial plafond covers two-thirds of the talar trochlear surface at the talocrural joint [3], and a larger radius of curvature of the tibial plafond than that of the talar trochlea has been observed at the lateral view of the ankle joint [16, 18]. The present study found that the tibial radius was significantly larger compared with the talar radius at both the mid and medial region of the talocrural joint. The larger tibial radius at the mid and medial region of the talocrural joint would permit the anteroposterior translation of the talus and the anteroposterior sliding motion of the medial compartment of the talar trochlea at the talocrural joint through the ankle range of motion. In particular, the largest gap of the radius between the tibial plafond and talar trochlea was found at the anteromedial region of the talocrural joint. This large gap would enable the combined motion of anterior rolling and posterior sliding at the talocrural joint during ankle dorsiflexion.

Our results indicate that the orientation patterns of the axis of rotation of the talocrural joint could be inferred by the asymmetry between anterior and posterior radii of the medial talar trochlea. Among the six regions of the talar trochlea, the anteromedial and posteromedial radius exhibited large individual variability, which resulted in the large variation in the medial APRR. The medial APRR then correlated with the mid APRR, anterior MLRR, and posterior MLRR. This indicates that the variation in the medial radius of the talar trochlea would determine the arthro-kinematics of the talocrural joint. In particular, when the medial APRR was small, the mid APRR and anterior MLRR were small whereas the posterior MLRR would be large. This type of the talus should exhibit the long mid and medial distances between the dorsiflexion and plantarflexion axes, the dorsiflexion axis orientating downward and laterally on the coronal plane and the plantarflexion axis orientating downward and medially, indicating a changing axis of rotation of the talocrural joint throughout the ankle range of motion [9]. Therefore, the talus that exhibits an extremely small anteromedial radius compared with the posteromedial radius, that is, a small medial APRR, would produce the large external rotation during both ankle dorsiflexion and plantarflexion and large anteroposterior translation of the talus with the large sliding motion of the medial talar compartment. On the other hand, the talus that has the anteromedial radius equivalent to the posteromedial radius, that is, a large medial APRR, should exhibit short mid and medial distances between the dorsiflexion and plantarflexion axes, the dorsiflexion and plantarflexion axis orientating slightly downward and laterally on the coronal plane, indicating a fixed axis of rotation of the talocrural joint throughout the ankle range of motion [9]. Therefore, the talus that exhibits a large medial APRR would produce a nearly pure sagittal backward rotation during ankle dorsiflexion and internal rotation during ankle plantarflexion, with few anteroposterior talar translations throughout the ankle range of motion.

In clinical settings, the subject-specific kinematics of the talocrural joint could be inferred by observing the asymmetry between the anterior and posterior radii of the medial talar trochlea using the lateral ankle view of the standard radiographic images. This would enable therapists to restore innate arthro-kinematics of the talocrural joint. For example, ankle range of motion is restricted postoperatively in patients with several ankle injuries, such as ankle fracture, ankle ligamentous injury, and osteochondral lesion of the talus. In these situations, if the patients exhibit a small anterior radius compared with the posterior radius at the medial trochlea on the lateral view of the ankle radiographic image, the anteroposterior translation of the mid talus and the sliding of the medial talar trochlea would need assistance from a therapist using manual therapy to improve the ankle dorsiflexion and plantarflexion range of motion. In addition, the postoperative timeline of exercise prescription for the patients with osteochondral lesion of the talus would need to be appropriately determined considering the individual asymmetry of the medial talar trochlea. Particularly, stage III osteochondral lesions of the talus are more likely located at the central third region of the medial trochlea [12]. After transplantation for this kind of osteochondral lesion, patients whose talus has a smaller anteromedial radius compared with the posteromedial radius would be susceptible to the shearing force at the site of the graft during weight-bearing ankle dorsiflexion and plantarflexion motion due to the larger talar translation and sliding relative to the tibial plafond. Therefore, for these patients, the starting period of such weight-bearing ankle motion should be delayed compared to patients whose talus has equivalent anteromedial and posteromedial radius to allow healing at the site of the graft. Furthermore, the detailed information about the radius of curvature at both the talar trochlea and tibial plafond would be beneficial for optimal design of total ankle replacements. In the future, the interaction between the asymmetric shape of the talar trochlea surface and kinematics of the talocrural joint should be demonstrated. Subsequently, the effects of the morphology of the talocrural joint surface on the mechanism of lateral ligamentous injuries [10], osteochondral lesions of the talus [17], and ankle osteoarthritis [14] should be determined.

Conclusions

The degrees of symmetry between anterior and posterior radii of the medial talar trochlea correlate with the asymmetry between both medial and lateral radii of the anterior and posterior talar trochlea. The asymmetric shape of the medial talar trochlea seems to determine the fixed or changing axis of rotation at the talocrural joint. This subject-specific

rotational axis of the talocrural joint should be considered in the management of patients with several kinds of ankle injuries.

Author contributions SN: Project development, data collection, data analysis, manuscript writing. KW: Data collection and management, manuscript editing. TK: Data collection, data analysis. TM: Data management, manuscript editing. TK: Data management, manuscript editing. MK: Project development, manuscript editing.

Compliance with ethical standards

Conflict of interest The authors have no conflict of interest with regard to this work.

References

1. Adam C, Eckstein F, Milz S, Putz R (1998) The distribution of cartilage thickness within the joints of the lower limb of elderly individuals. J Anat 193(Pt 2):203–214
2. Akiyama K, Sakai T, Sugimoto N, Yoshikawa H, Sugamoto K (2012) Three-dimensional distribution of articular cartilage thickness in the elderly talus and calcaneus analyzing the subchondral bone plate density. Osteoarthr Cartil 20:296–304. https://doi.org/10.1016/j.joca.2011.12.014
3. Armen SK, Shahan KS (2011) Sarrafian's anatomy of the foot and ankle: descriptive, topographic, functional, 3rd edn. Lippincott Williams & Wilkins, Philadelphia, pp 40–119
4. Barnett CH, Napier JR (1952) The axis of rotation at the ankle joint in man; its influence upon the form of the talus and the mobility of the fibula. J Anat 86:1–9
5. Imai K, Tokunaga D, Takatori R, Ikoma K, Maki M, Ohkawa H, Ogura A, Tsuji Y, Inoue N, Kubo T (2009) In vivo three-dimensional analysis of hindfoot kinematics. Foot Ankle Int 30:1094–1100. https://doi.org/10.3113/fai.2009.1094
6. Kitaoka HB, Luo ZP, An KN (1997) Three-dimensional analysis of normal ankle and foot mobility. Am J Sports Med 25:238–242
7. Latimer B, Ohman JC, Lovejoy CO (1987) Talocrural joint in African hominoids: implications for *Australopithecus afarensis*. Am J Phys Anthropol 74:155–175. https://doi.org/10.1002/ajpa.1330740204
8. Lundberg A, Goldie I, Kalin B, Selvik G (1989) Kinematics of the ankle/foot complex: plantarflexion and dorsiflexion. Foot Ankle 9:194–200
9. Lundberg A, Svensson OK, Nemeth G, Selvik G (1989) The axis of rotation of the ankle joint. J Bone Jt Surg Br 71:94–99
10. Magerkurth O, Frigg A, Hintermann B, Dick W, Valderrabano V (2010) Frontal and lateral characteristics of the osseous configuration in chronic ankle instability. Br J Sports Med 44:568–572. https://doi.org/10.1136/bjsm.2008.048462
11. Nozaki S, Watanabe K, Katayose M (2016) Three-dimensional analysis of talar trochlea morphology: implications for subject-specific kinematics of the talocrural joint. Clin Anat 29:1066–1074. https://doi.org/10.1002/ca.22785
12. Orr JD, Dutton JR, Fowler JT (2012) Anatomic location and morphology of symptomatic, operatively treated osteochondral lesions of the talus. Foot Ankle Int 33:1051–1057. https://doi.org/10.3113/FAI.2012.1051 doi
13. Portney LG, Watkins MP (2009) Foundations of clinical research: applications to practice. Pearson Prentice Hall, Upper Saddle River
14. Schaefer KL, Sangeorzan BJ, Fassbind MJ, Ledoux WR (2012) The comparative morphology of idiopathic ankle osteoarthritis. J Bone Jt Surg Am 94:e181. https://doi.org/10.2106/jbjs.l.00063
15. Siegler S, Toy J, Seale D, Pedowitz D (2013) New observations on the morphology of the talar dome and its relationship to ankle kinematics. Clin Biomech 29:1–6. https://doi.org/10.1016/j.clinbiomech.2013.10.009
16. Stagni R, Leardini A, Ensini A, Cappello A (2005) Ankle morphometry evaluated using a new semi-automated technique based on X-ray pictures. Clin Biomech 20:307–311. https://doi.org/10.1016/j.clinbiomech.2004.11.009
17. Tumer N, Blankevoort L, van de Giessen M, Terra MP, de Jong PA, Weinans H, Tuijthof GJ, Zadpoor AA (2016) Bone shape difference between control and osteochondral defect groups of the ankle joint. Osteoarthr Cartil 24:2108–2115. https://doi.org/10.1016/j.joca.2016.07.015
18. Wiewiorski M, Hoechel S, Wishart K, Leumann A, Muller-Gerbl M, Valderrabano V, Nowakowski AM (2012) Computer tomographic evaluation of talar edge configuration for osteochondral graft transplantation. Clin Anat 25:773–780. https://doi.org/10.1002/ca.22042
19. Yamaguchi S, Sasho T, Kato H, Kuroyanagi Y, Banks SA (2009) Ankle and subtalar kinematics during dorsiflexion–plantarflexion activities. Foot Ankle Int 30:361–366. https://doi.org/10.3113/FAI.2009.0361